Theory of Optical Parametric Noise

D. A. KLEINMAN
Bell Telephone Laboratories, Murray Hill, New Jersey 07971
(Received 5 March 1968)

Optical parametric noise (OPN) is treated as a quantum-mechanical decay process in which a photon ω_3 decays in an optically nonlinear medium into two photons ω_1, ω_2. The correct form of the interaction Hamiltonian is derived in terms of the usual second-order susceptibility, the field is quantized in a simple way, and the transition rate is obtained for an arbitrary field distribution at ω_3. It is shown that focusing does not enhance OPN. The properties of OPN are then described in considerable detail for a plane wave at ω_3 using a rigorous treatment of the crystal optics. OPN will usually be dominated by processes which very nearly conserve momentum and which produce a narrow-band emission whose frequency is determined by the direction of emission. Also considered is the background due to momentum-nonconserving processes, which produce broad-band emission up to a sharp cutoff frequency which depends on the emission direction. Appendices are provided on the group velocity in crystals, the "noise-wave" theory of OPN, second-harmonic generation, and OPN with beams of finite cross section.

1. INTRODUCTION

OPTICAL parametric noise (OPN), also known as parametric fluorescence[1] or spontaneous parametric interaction,[2] is radiation emitted in an optically nonlinear crystal due to the spontaneous decay of a photon ω_3 into two photons ω_1, ω_2:

$$\omega_3=\omega_1+\omega_2, \tag{1}$$

where $\omega=2\pi\nu$ is the angular frequency. The greatest emission occurs when conservation of momentum (phase matching) can also be satisfied:

$$\mathbf{k}_3=\mathbf{k}+\mathbf{j}, \tag{2}$$

where $\mathbf{k}$, $\mathbf{j}$, $\mathbf{k}_3$ are wave vectors at ω_1, ω_2, ω_3, respectively. OPN satisfying (1) and (2) has been observed[1–7] and may prove valuable[1,4] as a tunable source of radiation and as a technique for measuring the nonlinear optical coefficients of crystals. It is also the main source of noise in low-gain optical parametric amplifiers and frequency converters employing a laser pump at ω_3.

The theory of OPN is in need of clarification because of several different approaches in the literature and drastically different results which have not been reconciled. The notion most often employed[1,2,5] is that OPN is due to *parametric amplification* by the pump of a fictitious "zero-point" power $h\nu_1 d\nu_1$ in bandwidth $d\nu_1$; after amplification the original "zero-point" power is subtracted off and the remainder is assumed to be observable as OPN. Results obtained with the assumption of fictitious powers, although possibly of interest, must certainly be considered tentative. Another notion[4] employing fictitious powers is that OPN is a *mixing* process in which "zero-point" power of one photon $\hbar\omega_2$ per mode mixes with the pump ω_3 to produce the observed OPN at ω_1. One might be tempted to add the contributions from parametric amplification and parametric mixing. Actually, both contributions appear in a consistent treatment (Appendix B) of the parametric interaction of two "noise waves" with the pump. It is necessary to allow for arbitrary initial conditions, arbitrary mismatch Δk, and arbitrarily small gain compared to Δk; the correct answer then results from assuming the correct zero-point energy $\frac{1}{2}\hbar\omega$ in each mode. It is also true (although hardly obvious in advance) that the correct answer can be obtained by either of two arbitrary procedures in which (a) one neglects mixing, and the energy $\hbar\omega$ per mode is assumed to be amplified, or (b) one neglects amplification and assumes that energy $\hbar\omega$ per mode mixes with the pump.

The direct way[8] to calculate OPN, which makes no use of fictitious powers, is by means of quantum-mechanical perturbation theory. In this method one obtains the transition rate for the decay $\omega_3\rightarrow\omega_1+\omega_2$ using an interaction energy proportional to the nonlinear susceptibility. In this method it is important to derive the interaction with care, because confusion can arise between interactions of the form $\int\mathbf{E}\cdot d\mathbf{P}$ and $-\int\mathbf{P}\cdot d\mathbf{E}$, where $\mathbf{E}$ is the field and $\mathbf{P}$ is the (nonlinear) polarization. As a check, one can compute the second-harmonic generation from the transition rate (Appendix C). Recently, Giallorenzi and Tang[9] have given a detailed quantum-mechanical treatment in which they prove that OPN is independent of the coherence of the

[1] S. E. Harris, M. K. Oshman, and R. L. Byer, Phys. Rev. Letters **18**, 732 (1967). Equation (1) is incorrect.
[2] D. Magde and H. Mahr, Phys. Rev. Letters **18**, 905 (1967). Equation (2) is incorrect.
[3] D. Magde, R. Scarlet, and H. Mahr, Appl. Phys. Letters **11**, 381 (1967).
[4] R. L. Byer and S. E. Harris, Phys. Rev. **168**, 1064 (1968). Results embodied in (5), (6), and (8) are correct.
[5] R. G. Smith, J. G. Skinner, J. E. Geusic, and W. G. Nilsen, Appl. Phys. Letters **12**, 97 (1968). Equation (4) is too small by a factor of 2.
[6] S. Akhmanov, V. Fadeev, R. Khokhlov, and O. Chunaev, Zh. Eksperim. i Teor. Fiz. Pis'ma v Redaktsiyu **6**, 575 (1967) [English transl.: JETP Letters **6**, 85 (1967)].
[7] C. H. Henry and J. J. Hopfield, Phys. Rev. Letters **15**, 964 (1965); W. L. Faust and C. H. Henry, *ibid.* **17**, 1265 (1966). The Raman scattering of the polariton is an example of OPN if the polariton is regarded as a photon propagating in an extremely dispersive region of the spectrum.
[8] D. N. Klyshko, Zh. Eksperim. i Teor. Fiz. Pis'ma v Redaktsiyu **6**, 490 (1967) [English transl.: JETP Letters **6**, 23 (1967)]. Equation (1) is too small by a factor of 4 and should not contain $\cos\nu_1$.
[9] T. G. Giallorenzi and C. L. Tang, Phys. Rev. **166**, 225 (1968).

pump beam. Their final result, Eq. (35) of Ref. 9, however, varies inversely with the solid angle $\Delta\Omega_3$ of the pump and therefore is awkward to apply to a plane-wave pump ($\Delta\Omega_3=0$). This happened because they tacitly assumed $\Delta\Omega_3$ to be much larger than angular effects dependent on the finite length of the crystal. It is the opposite case (plane-wave pump, $\Delta\Omega_3=0$) that exhibits the most interesting and significant features.

None of the theories mentioned is valid for large dispersion; they all make the approximation that the group velocity equals the phase velocity. The case of large dispersion is very interesting, however, because large dispersion and large nonlinear coefficients often go together.[7] Dispersion together with the optical anisotropy of the crystal can be treated rigorously by means of the vector group velocity $\mathbf{v}\equiv\nabla\omega(\mathbf{k})$.

In this paper, the transition rate for OPN is obtained from perturbation theory using a Hamiltonian and quantum conditions that are correct in the presence of dispersion and anisotropy. The perturbation theory is checked by verifying that it gives the correct second-harmonic generation. It is shown that OPN is not enhanced by focusing (unlike harmonic generation), as one might expect from its independence of the coherence[9] of the pump beam. A compact expression is obtained for the angular and spectral distribution of OPN power for the case of a plane-wave pump and a crystal slab of finite thickness but arbitrarily large area (actually it is only required that the slab be larger than the beam). The properties of phase-matched OPN are described in considerable detail by means of the concept of the matching surface. A detailed description is also given of the mismatched background OPN. A systematic development of the theory of the group velocity in anisotropic dispersive crystals, which does not seem to be readily available in the literature, is given in Appendix A. In Appendix B is given a treatment of OPN based on the parametric interaction of "noise waves" with the pump. This consistent treatment reconciles and unifies the parametric amplification and mixing approaches to OPN. The correct (perturbation-theory) result is obtained when the noise waves have the zero-point energy $\frac{1}{2}\hbar\omega$ per mode. Appendix C shows that the interaction used here gives the correct second-harmonic generation. In Appendix D, an explicit condition is obtained for the validity of treating a finite pump beam as a plane wave.

2. FORMULATION OF THE THEORY

The system is an electromagnetic field in an arbitrarily large volume $V=L^3$ containing nonabsorptive material. Within V is a smaller volume $W=L^2l$ in the shape of a slab of thickness l in which there is a second-order polarization $\mathbf{P}$ of the general form[10]

$$\mathbf{P}_2(\mathbf{r})=\chi(-\omega_2,-\omega_1,\omega_3):\mathbf{E}_1(\mathbf{r})^*\mathbf{E}_3(\mathbf{r}), \tag{3}$$

where $\mathbf{E}_1(\mathbf{r})$ is the complex vector amplitude of the field at ω_1 defined by

$$\mathbf{E}_1(\mathbf{r},t)=\mathrm{Re}[\mathbf{E}_1(\mathbf{r})e^{-i\omega_1 t}]. \tag{4}$$

The tensor commonly used to describe second-harmonic generation[11] is $\mathbf{d}=\frac{1}{2}\chi(-2\omega,\omega,\omega)$. The contribution of χ to the energy of the medium is

$$\int_W d\mathbf{r}\int_0^P \mathbf{E}\cdot d\mathbf{P}.$$

This, however, is not the interaction energy relevant for OPN, since in the unperturbed field $\mathbf{P}(\mathbf{r})=0$. Therefore we must start at $\mathbf{P}=0$ and turn on $\mathbf{P}$ adiabatically at constant $\mathbf{E}$, then change $\mathbf{E}$ and $\mathbf{P}$ according to (3), and finally reduce $\mathbf{P}$ adiabatically at constant $\mathbf{E}$ to $\mathbf{P}=0$. The work done by the field in this process is

$$H'=-\int_W d\mathbf{r}\int_0^E \mathbf{P}\cdot d\mathbf{E}, \tag{5}$$

which is the correct interaction energy for OPN. It is convenient, though not essential to our treatment, to assume that dispersion in χ can be neglected; then χ possesses sufficient symmetry[12] that (5) can be written in the simple form

$$H'=-\tfrac{1}{3}\int_W d\mathbf{r}\,\mathbf{E}\cdot\chi:\mathbf{E}\mathbf{E}, \tag{6}$$

where $\mathbf{E}=\mathbf{E}(\mathbf{r},t)$ is the sum of all fields present. Introducing the field amplitudes defined by (4) and neglecting the rapidly oscillating parts of H' gives

$$\begin{aligned} H'&=-\tfrac{1}{4}\int_W d\mathbf{r}[\mathbf{E}_3(\mathbf{r})\cdot\chi:\mathbf{E}_1(\mathbf{r})^*\mathbf{E}_2(\mathbf{r})^*+\text{c.c.}] \\ &=-\tfrac{1}{4}\chi\int_W d\mathbf{r}[E_3(\mathbf{r})E_1(\mathbf{r})^*E_2(\mathbf{r})^*+\text{c.c.}], \end{aligned} \tag{7}$$

where the fields $E_j(\mathbf{r})$ are now scalar amplitudes and the polarization directions of the fields are taken into account in the effective nonlinear coefficient χ. Moreover, it is convenient to define $E_j(\mathbf{r})$ as the amplitude of the *transverse* component of the field. Thus, if $\mathbf{s}$ is a unit vector in the propagation direction and $\mathbf{u}$ is a unit vector in the field direction, the vector field is

$$\mathbf{E}(\mathbf{r})=\mathbf{u}E(\mathbf{r})\csc(\mathbf{u},\mathbf{s}) \tag{8}$$

and the effective nonlinear coefficient is

$$\chi=\mathbf{u}_3\cdot\chi:\mathbf{u}_1\mathbf{u}_2\csc(\mathbf{u}_3,\mathbf{s}_3)\csc(\mathbf{u}_1,\mathbf{s}_1)\csc(\mathbf{u}_2,\mathbf{s}_2). \tag{9}$$

If the dependence of χ on ω_1, ω_2 is important, (7)

[10] J. A. Armstrong, N. Bloembergen, J. Ducuing, and P. Pershan, Phys. Rev. 127, 1918 (1962).

[11] D. A. Kleinman, Phys. Rev. 128, 1761 (1962).

[12] D. A. Kleinman, Phys. Rev. 126, 1977 (1962).

remains valid[13] although the more general derivation [not using (6)] will not be given here.

We expand the fields at ω_1, ω_2 in plane waves but allow the laser field to have a general form specified by $f(\mathbf{r})$. Thus we write

$$\begin{aligned} E_1(\mathbf{r}) &= \sum_k E_k e^{i\mathbf{k}\cdot\mathbf{r}}, \\ E_2(\mathbf{r}) &= \sum_j E_j e^{i\mathbf{j}\cdot\mathbf{r}}, \\ E_3(\mathbf{r}) &= E_3 f(\mathbf{r}), \\ \int_V |f(\mathbf{r})|^2 d\mathbf{r} &= V. \end{aligned} \tag{10}$$

The wave vectors $\mathbf{k}$, $\mathbf{j}$ at ω_1, ω_2, respectively, satisfy periodic boundary conditions in V. At each frequency we shall quantize the field by imposing a commutation condition of the form

$$[E,E^\dagger]=C, \tag{11}$$

where the E, $E^\dagger$ are now operators and C is a constant. The classical energy density in a lossless medium with dispersion and anisotropy is [see Eq. (A27)]

$$U=(nc/8\pi v)|E|^2, \tag{12}$$

where $v\equiv\mathbf{v}\cdot\mathbf{s}$ is the component of the *group velocity*[14] in the propagation direction, n is the refractive index, and E is the transverse component of the field. We therefore write, for the Hamiltonian of the noninteracting field at one frequency,

$$H=V(nc/8\pi v)E^\dagger E \tag{13}$$

and choose C in (11) such that the eigenvalues of H are $N\hbar\omega$, where $N=0, 1, 2, \cdots$. In this way we are led to the quantum conditions

$$\begin{aligned} [E_k,E_{k'}{}^\dagger] &= (8\pi\hbar\omega_1 v_1/cn_1V)\delta_{kk'}, \\ [E_j,E_{j'}{}^\dagger] &= (8\pi\hbar\omega_2 v_2/cn_2V)\delta_{jj'}, \\ [E_3,E_3{}^\dagger] &= (8\pi\hbar\omega_3 v_3/cn_3V), \end{aligned} \tag{14}$$

with all other commutators vanishing.

The only assumption we make at this time concerning the laser field $f(\mathbf{r})$ is that the surfaces of constant phase should propagate in one direction normal to the slab. This rules out standing waves such as would result from reflecting surfaces that were not perpendicular to the slab. It follows that, parallel to the slab, $f(\mathbf{r})$ does not propagate but describes some stationary distribution such as a Gaussian beam, a higher-order transverse mode of a laser cavity, or a standing wave pattern produced by reflecting surfaces perpendicular to the slab. A special case of great theoretical interest is when $f(\mathbf{r})$ is a plane wave normal to the slab. We make the aforementioned assumption about $f(\mathbf{r})$ in order to be able to relate the quantum number N of the laser mode to the power $\mathcal{P}_3$ incident on the slab:

$$\mathcal{P}_3=\hbar\omega_3(v_3/L)N. \tag{15}$$

This relation also holds if N is the average photon number of the laser mode in a nonstationary state such as the so-called coherent states.[15] For simplicity, we shall assume that the laser mode is in a quantum state N, since the transition rate for OPN is independent of the coherence of the field.[9]

The interaction Hamiltonian (7) can now be written

$$H'=-\tfrac{1}{4}\sum_k\sum_j \chi[f(\mathbf{k}+\mathbf{j})E_3E_k{}^\dagger E_j{}^\dagger+\text{c.c.}], \tag{16}$$

where

$$f(\mathbf{K})\equiv\int_W d\mathbf{r}\, f(\mathbf{r})e^{-i\mathbf{K}\cdot\mathbf{r}} \tag{17}$$

may be considered as a Fourier amplitude of the laser field (with respect to the slab volume W). The transition $|0,0,N\rangle\rightarrow|\mathbf{k},\mathbf{j},N-1\rangle$ creates photons in states $\mathbf{k}$, $\mathbf{j}$ and destroys a photon in state $f(\mathbf{r})$. The rate for this transition is[16]

$$\begin{aligned} R&=(2\pi/\hbar^2)\delta(\omega_3-\omega_1-\omega_2)|\langle N,0,0|H'|\mathbf{k},\mathbf{j},N-1\rangle|^2 \\ &=(2^6\pi^4/c^3n_3L^8)\mathcal{P}_3\chi^2|f(\mathbf{k}+\mathbf{j})|^2(v_1v_2\omega_1\omega_2/n_1n_2) \\ &\quad\times\delta(\omega_3-\omega_1-\omega_2). \end{aligned} \tag{18}$$

Note that R does not depend on the relative phases of the Fourier amplitudes $f(\mathbf{k}+\mathbf{j})$. Thus OPN can not be enhanced by focusing, and for a focused beam it is independent of the position of the focus. This sharply distinguishes OPN from second-harmonic generation which is sensitive to focusing.[17–19] We shall assume that photon $\mathbf{k}$ is observed experimentally and $\mathbf{j}$ is not observed. Therefore we must sum over all $\mathbf{j}$ for which $R\neq0$. We also sum over certain values of $\mathbf{k}$ which fall within some frequency band $\Delta\nu_1$ and solid-angle window $\Delta\Omega_1$. The sum over $\mathbf{k}$ of any quantity Q can be written as an integral:

$$\sum_k Q=(2\pi)^{-3}V\int\int Qk^2dkd\Omega_1. \tag{19}$$

It follows from the definition of v_1 that $d\omega_1=v_1dk$ (see Appendix A). Thus the observed power $\Delta\mathcal{P}_1$ in $\Delta\nu_1$ and $\Delta\Omega_1$ is

$$\begin{aligned} \Delta\mathcal{P}_1=\sum_j\sum_k R\hbar\omega_1&=\Delta\nu_1\Delta\Omega_1\hbar\omega_1(2\pi)^{-5}V^2(k^2/v_1) \\ &\quad\times\int\int\int dj_xdj_ydj_zR \end{aligned} \tag{20}$$

[13] P. S. Pershan, Phys. Rev. **130**, 919 (1963).
[14] L. Brillouin, *Wave Propagation and Group Velocity* (Academic Press Inc., New York, 1960).
[15] R. J. Glauber, Phys. Rev. **131**, 2766 (1963). See also Ref. 22.
[16] See any text on quantum mechanics, for example, L. I. Schiff, *Quantum Mechanics* (McGraw-Hill Book Co., New York, 1949), Sec. 29.
[17] D. A. Kleinman, A. Ashkin, and G. D. Boyd, Phys. Rev. **145**, 338 (1966).
[18] J. E. Bjorkholm, Phys. Rev. **142**, 126 (1966).
[19] D. A. Kleinman and R. C. Miller, Phys. Rev. **148**, 302 (1966).

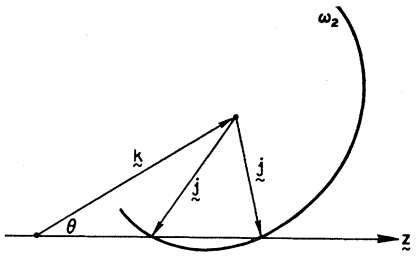

FIG. 1. A general OPN process satisfying (1) and (23) but not (2). The laser beam is in the direction **z** and the photons emitted have frequencies ω_1, ω_2 and wave vectors **k**, **j**. In general, there are two possible **j** if **k** is fixed. The curve ω_2 represents all possible photons of frequency ω_2 which can propagate in the crystal, and the allowed **j** are the intersections of this surface with **z**.

and $k=n_1\omega_1/c$. This treatment is valid only when stimulated decay processes can be neglected. Thus we require $Rt\ll 1$, where t is the transit time of a photon across the slab. This is the case of *small parametric gain*. Also, losses have been neglected.

3. OPN FOR A PLANE-WAVE LASER BEAM

If the beam ω_3 is a plane wave in the z direction normal to the slab, we have, from (17),

$$|f(\mathbf{k}+\mathbf{j})|^2=(2\pi L)^2\delta(k_x+j_x)\delta(k_y+j_y)\times[\sin^2(\tfrac{1}{2}\Delta kl)/(\tfrac{1}{2}\Delta k)^2], \quad (21)$$

with

$$\Delta k\equiv n_3\omega_3/c-k_z-j_z. \quad (22)$$

It follows that

$$k_x+j_x=k_y+j_y=0, \quad (23)$$

which, together with (1), determines **j** as a continuous function of **k**. Figure 1 shows **k** at angle θ to the z direction. Using the end of **k** as center, a surface can be constructed $\omega_2(\mathbf{j})=\omega_3-\omega_1$, which is the locus of all **j** satisfying (1). This surface intersects **z** at two points which satisfy (23). Both of these are allowed processes, but ordinarily it is permissible to retain only the one with the smaller value of $|\Delta k|$. However, this is not the case in the degenerate situation shown in Fig. 2. Here, the ω_2 surface just touches the z direction at a single tangent point **j**. It is clear that if ω_1 were to be increased no solution of (1) and (23) would exist. Therefore the surface labelled ω' is the locus of maximum frequencies observable in any direction θ. Also indicated in Fig. 2 is the group velocity $\mathbf{v}_2=\mathbf{v}(\mathbf{j})$, where

$$\mathbf{v}(\mathbf{j})\equiv\nabla_j\omega(\mathbf{j}). \quad (24)$$

Note that we do not define v_2 as $|v_2|$ but $v_2\equiv\partial\omega/\partial j$. In general, **v** is normal to any surface $\omega=$ const and therefore is normal to **z** in Fig. 2. A property of the *limit surface* ω' is that all processes on ω' have $v_{2z}=0$.

We assume that the photon ω_1, **k** is observed in a definite allowed polarization direction. For each **j** there are two distinct processes corresponding to the two polarization directions for the unobserved photon ω_2, **j**. An exception is when $\chi=0$ for one of these polarizations. We shall write expressions for the contribution to the OPN from a single **j** and a single polarization (with due care in the special case $v_{2z}=0$); all contributions have the same general form, and it must be decided in each application if several contributions need to be added together. From (20), (21), and (24), it follows that the *power* $\Delta\mathcal{P}_1$ emitted into a spectrometer having arbitrarily small solid angle $\Delta\Omega_1$ and frequency ($\nu=\omega/2\pi$) bandwidth $\Delta\nu_1$ is ($\omega_1<\omega'$)

$$\Delta\mathcal{P}_1=\Delta\nu_1\Delta\Omega_1\cdot\frac{8\pi\mathcal{P}_3h}{n_3c^5}\cdot\frac{\chi^2n_1v_2\omega_1^4\omega_2}{n_2|v_{2z}|}\cdot\frac{\sin^2(\frac{1}{2}\Delta kl)}{(\frac{1}{2}\Delta k)^2}. \quad (25)$$

Only the third and fourth factors depend on the particular **k**, **j** process being observed. For $\omega_1>\omega'(\theta)$ we have $\Delta\mathcal{P}_1=0$.

Equation (25) is the basic result of the theory, and forms the starting point for our deductions about the properties of OPN. Our derivation treats the optical anisotropy and dispersion rigorously by means of the concept of the group velocity **v**. Since the formal properties of **v** are not readily available in the standard

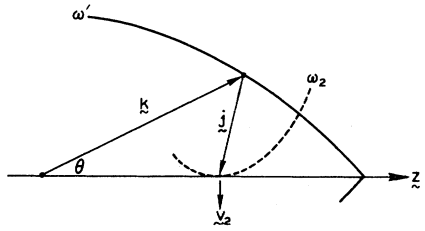

FIG. 2. A typical process at the limiting frequency $\omega_1=\omega'(\theta)$. The limit surface ω' is the locus of those **k** for which the ω_2 surface just touches **z**. All allowed processes must lie inside or on ω'. Also shown is the group velocity $\mathbf{v}_2$, which, for a limit process, is normal to **z**.

treatises on optics, we have given a brief discussion in Appendix A.

4. PHASE-MATCHED OPN

The function of Δk in (25) is familiar from the theory of harmonic generation,[11] where it is customary to regard $2\pi/\Delta k$ as the coherence length over which the laser and harmonic fields remain in phase. Only a limited number of nonlinear crystals permit phase matching ($\Delta k=0$) for harmonic generation. In the present case, however, there will always be some combinations ω_1, ω_2 satisfying (1) that permit $\Delta k=0$. The condition $\Delta k=0$ defines the *matching surface*. Figure 3 shows a typical matching surface for the case $\omega_1>\omega_2$. When $v_{2z}=0$, the matching surface is tangent to the limit surface. We may regard Δk as a function of **k**; it follows from (22)–(24) that an arbitrary variation $\delta\mathbf{k}$ produces the variation $\delta\Delta k$ given by

$$v_{2z}\delta\Delta k=\delta\mathbf{k}\cdot(\mathbf{v}_1-\mathbf{v}_2). \quad (26)$$

This shows that $\mathbf{v}_1-\mathbf{v}_2$ is in the direction normal to the

matching surface. Unless it is very small, the matching surface will dominate the OPN, giving rise to a narrow-band emission whose center frequency depends on the direction of $\mathbf{k}$. When $\omega_1>\omega_2$ as in Fig. 3, there will be two narrow-band emissions corresponding to the two intersections of the observation direction with the surface; there will also be a third emission $\omega_1<\omega_2$ coming from a part of the matching surface (not shown) enclosing $k=0$. Considering only one of these, we may integrate (25) over ν_1 to obtain the *total power* emitted in $\Delta\Omega_1$:

$$\frac{\Delta\mathcal{P}_1}{\Delta\Omega_1}=\frac{8\pi\mathcal{P}_3\hbar l}{n_3c^5}\frac{\chi^2n_1v_1v_2\omega_1^4\omega_2}{n_2|\mathbf{s}_1\cdot(\mathbf{v}_1-\mathbf{v}_2)|}, \tag{27}$$

where $\mathbf{s}_1=\mathbf{k}/k$ denotes the observation direction. It is not important whether we regard $\mathbf{s}_1$ or the direction of $\mathbf{v}_1$ as the observation direction, since one direction can always be determined if the other is known. The integration over ν_1 was carried out by means of the relation

$$\partial\Delta k/\partial\nu_1=(2\pi/v_1v_{2z})[\mathbf{s}_1\cdot(\mathbf{v}_1-\mathbf{v}_2)], \tag{28}$$

which follows from (26).

The *effective bandwidth* of the emission may be defined as the frequency band for which

$$|\Delta k|\leq\pi/l, \tag{29}$$

which gives

$$\Delta\nu=v_1|v_{2z}|\,|\mathbf{s}_1\cdot(\mathbf{v}_1-\mathbf{v}_2)|^{-1}l^{-1}. \tag{30}$$

It is assumed here that $\Delta\Omega_1$ is sufficiently small that the spread of center frequencies can be neglected. It follows from (30) that (27) may be written

$$\frac{\Delta\mathcal{P}_1}{\Delta\Omega_1}=\Delta\nu\frac{8\pi\mathcal{P}_3\hbar\chi^2n_1v_2\omega_1^4\omega_2}{n_2n_3c^5|v_{2z}|}l^2. \tag{31}$$

We note from (25) that the emission becomes very intense at the line center as $v_{2z}\to0$; however, (30) shows that the bandwidth becomes very small as $v_{2z}\to0$; the result is that the integrated line strength (27) does not depend on v_{2z}. Although we shall not give the details here, (26) can be continued to include second-order terms in $\delta\mathbf{k}\delta\mathbf{k}$ and $\delta\mathbf{j}\delta\mathbf{j}$, where $\delta\mathbf{j}=-\delta\mathbf{k}-\mathbf{z}\delta\Delta k$ ($\mathbf{z}$ a unit vector). When $v_{2z}=0$, it can easily be shown that

$$\Delta\nu=\frac{\pi v_1|\mathbf{zz}:\nabla\mathbf{v}_2|}{4|\mathbf{s}_1\cdot(\mathbf{v}_1-\mathbf{v}_2)|l^2}.$$

Thus the bandwidth (although nonvanishing) becomes so narrow that the integrated line strength is independent of l when $v_{2z}=0$. This case is best regarded as part of the $\Delta k\neq0$ background which will be discussed in Sec. 6. Generally speaking, we expect that only processes giving an integrated line strength proportional to l will be readily observable experimentally.

An interesting feature of the $\Delta k=0$ process occurs when $\mathbf{s}$ just glances the edge of the surface; there is then only one emission $\omega_1>\omega_2$ corresponding to the point of tangency. As this condition is approached we have $\mathbf{s}_1\cdot(\mathbf{v}_1-\mathbf{v}_2)\to0$; it follows from (27) and (30) that both power and bandwidth should greatly increase. By supplementing (26) with terms in $\delta\mathbf{k}\delta\mathbf{k}$ it can be shown that

$$\partial\Delta k/\partial\nu_1=(2\pi/v_1v_{2z})|2v_{2z}\mathbf{s}_1\mathbf{s}_1:\nabla(\mathbf{v}_1+\mathbf{v}_2)|^{1/2}(\Delta k)^{1/2}\quad[\mathbf{s}_1\cdot(\mathbf{v}_1-\mathbf{v}_2)=0]. \tag{32}$$

By means of this relation (25) can be integrated over ν_1 to obtain the *edge power* ($\omega_1>\omega_2$):

$$\frac{\Delta\mathcal{P}_1}{\Delta\Omega_1}=\frac{8\pi\mathcal{P}_3\hbar l^{3/2}I}{n_3c^5}\frac{\chi^2n_1v_1v_2\omega_1^4\omega_2}{n_2|v_{2z}\mathbf{s}_1\mathbf{s}_1:\nabla(\mathbf{v}_1+\mathbf{v}_2)|^{1/2}}, \tag{33}$$

where I is the integral

$$I=\int_0^\infty\frac{dz}{\pi z^{5/2}}\sin^2z\approx0.8. \tag{34}$$

The effective bandwidth of the emission from the edge is

$$\Delta\nu=|2v_{2z}v_1^2/\pi l|^{1/2}|\mathbf{s}_1\mathbf{s}_1:\nabla(\mathbf{v}_1+\mathbf{v}_2)|^{-1/2}. \tag{35}$$

Equating (27) and (33) gives the criterion

$$|\mathbf{s}_1\cdot(\mathbf{v}_1-\mathbf{v}_2)|<I^{-1}|(v_{2z}/l)\mathbf{s}_1\mathbf{s}_1:\nabla(\mathbf{v}_1+\mathbf{v}_2)|^{1/2} \tag{36}$$

for the validity of (33) and (35). We see in (33) that the peak power reached at the edge varies as $l^{3/2}$ compared with l for the normal processes (27). Thus the magnitude of the *enhancement* as the edge is approached depends on l. In a sufficiently long crystal there would be a pronounced enhancement at the edge accompanied by a broader effective bandwidth (35) varying as $l^{-1/2}$ compared with l^{-1} for normal processes. From (26) and (36) it follows that the angular width $\Delta\theta$ of the edge peak is

$$\Delta\theta=2I^{-1}|\mathbf{v}_1-\mathbf{v}_2|^{-1}|(v_{2z}/l)\mathbf{s}_1\mathbf{s}_1:\nabla(\mathbf{v}_1+\mathbf{v}_2)|^{1/2}. \tag{37}$$

Since $\Delta\theta\sim l^{-1/2}$ while $\Delta\mathcal{P}_1/\Delta\Omega_1\sim l^{3/2}$, it follows that the total edge power integrated over $\Delta\Omega_1$ varies as l. The

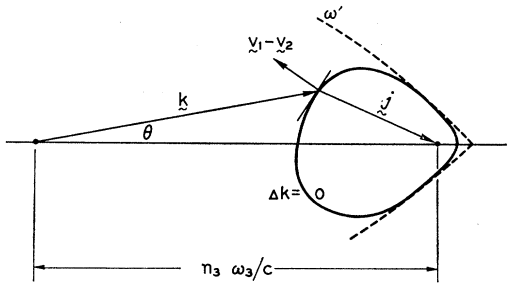

FIG. 3. A typical phase-matched process in which $\mathbf{k}$ lies on the matching surface $\Delta k=0$. Also shown is $\mathbf{v}_1-\mathbf{v}_2$, which is normal to the matching surface. In the case drawn $\omega_1>\omega_2$, there are two combinations $\mathbf{k}$, $\mathbf{j}$ which could give emission in the direction θ, only one of which is shown. There is also one emission with $\omega_1<\omega_2$.

edge power (33) can be written in the form (31) with $\Delta\nu$ the effective band (35).

Another special case of enhancement and line broadening formally identical with the edge process just treated is the *degenerate process* when $\mathbf{v}_1=\mathbf{v}_2$. If $\mathbf{k}$ and $\mathbf{j}$ have the same polarization direction, this would imply $\omega_1=\omega_2$ and $\theta=0$. There is an enhancement as the degenerate case is approached, since

$$|\mathbf{s}_1\cdot(\mathbf{v}_1-\mathbf{v}_2)|\rightarrow 0.$$

The degenerate peak power is given by (33) with $\mathbf{v}_1=\mathbf{v}_2$ and $\Delta\nu$ is given by (35). The angular width of the degenerate peak is

$$\Delta\theta=(2c/n_1\omega_1)|(\pi v_{2z}/l)|^{1/2}|\mathbf{tt}:\nabla\mathbf{v}|^{-1/2}, \tag{38}$$

where $\mathbf{t}$ is a unit vector transverse to $\mathbf{z}$ in the plane in which θ is measured. Again we see that the enhanced region contributes an integrated power (over $\Delta\Omega_1$) which varies as l.

Up to this point, we have made no approximations concerning the dispersion or anisotropy of the crystal. The computation of the matching surface requires an exact treatment of these optical properties. However, this rigor may be unnecessary in the computation of the various factors containing $\mathbf{v}$ and $\nabla\mathbf{v}$ that have appeared in the theory. In the approximation of an isotropic medium with dispersion, we have

$$\begin{aligned} v&\equiv\partial\omega/\partial k\approx c/[n+\omega(\partial n/\partial\omega)],\\ \mathbf{v}&\equiv\nabla\omega\approx v\mathbf{s},\\ \nabla\mathbf{v}&\approx(c^2/n^2\omega)[(\mathbf{1}-\mathbf{ss})-(2\omega/n)(\partial n/\partial\omega)\mathbf{ss}], \end{aligned} \tag{39}$$

where $\mathbf{1}$ is the unit dyadic.

The total power $\mathcal{P}_1$ of phase-matched OPN is of interest in the case $\omega_1\gg\omega_2$, where the emission is confined to a rather small solid angle and a bandwidth of order ω_2. Under these conditions, $\mathcal{P}_1$ is apt to reach the detector. In (27) we may interchange subscripts 1,2 to obtain $\Delta\mathcal{P}_2/\Delta\Omega_2$. If $\omega_2<\omega_1$, there is no edge enhancement to contend with, and (27) is valid at all angles. Each increment $\Delta\mathcal{P}_2$ corresponds to a detected increment of power $\Delta\mathcal{P}_1=(\omega_1/\omega_2)\Delta\mathcal{P}_2$. Thus the *total phase-matched power* is

$$\mathcal{P}_1=\frac{8\pi\mathcal{P}_3hl}{n_3c^5}\frac{v_1}{n_1}\int\frac{\chi^2n_2v_2\omega_2^3\omega_1^2d\Omega_2}{|\mathbf{s}_2\cdot(\mathbf{v}_2-\mathbf{v}_1)|}, \tag{40}$$

where we have recognized that v_1/n_1 can be considered constant when the matching surface is very small. It is reasonable to suppose that $\mathcal{P}_1$ is not sensitive to the detailed optical properties of the crystal. Therefore we neglect both anisotropy and dispersion; it can then be shown that when $\Delta k=0$,

$$\begin{aligned} \omega_2(\theta_2)&=\omega_3(n_1-n_3)/(n_1-n_2\cos\theta_2),\\ |\mathbf{s}_2\cdot(\mathbf{v}_2-\mathbf{v}_1)|&=(c/n_1n_2)(n_1-n_2\cos\theta_2), \end{aligned} \tag{41}$$

where n_1, n_2, and n_3 are constant refractive indices satisfying $n_1>n_3$, $n_1>n_2$. The integral (40) is dominated by the forward region $\theta_2\sim0$ because of the factor ω_2^3. Therefore, χ^2 and ω_1^2 can be assigned values appropriate to $\theta_2=0$. The integral can be evaluated to give ($\omega_1\gg\omega_2$)

$$\mathcal{P}_1\approx\frac{16\pi^2\mathcal{P}_3hl\chi^2\omega_1^2\omega_2^3}{3n_3n_1c^4}, \tag{42}$$

where $\omega_2=\omega_2(0)$; the integration also gives a second term containing $\omega_2(\pi)^3$ which can be neglected.

5. TYPES OF MATCHING SURFACE

The matching surface (MS) shown in Fig. 3 is only one of several possible types. It is convenient to refer to the ends of the pump wave vector $n_3\omega_3/c$ as foci, which are indicated as heavy dots in Fig. 3. Assume for simplicity that ω_1 and ω_2 are both ordinary waves in a uniaxial crystal and ω_3 is an extraordinary wave. The vector diagram for the matching case (2) shown in Fig. 3 requires

$$\omega_2n_2=+[(\omega_3n_3)^2+(\omega_1n_1)^2-2\omega_3n_3(\omega_1n_1)\cos\theta]^{1/2}. \tag{43}$$

Processes with $\theta=0$ (or π) are called *collinear*; collinear processes may be further classified as *forward wave* (FW) satisfying

$$n_1\omega_1+n_2\omega_2=n_3\omega_3 \quad (\text{FW}) \tag{44}$$

and *backward wave* (BW) satisfying

$$n_1\omega_1-n_2\omega_2=n_3\omega_3 \quad (\text{BW}). \tag{45}$$

Another BW process has $\theta=\pi$:

$$n_2\omega_2-n_1\omega_1=n_3\omega_3 \quad (\text{BW}). \tag{46}$$

Figure 4(a) shows a schematic plot of $n_1\omega_1$ and $n_2\omega_2=[n(\omega_3-\omega_1)](\omega_3-\omega_1)$ with the curvature somewhat exaggerated to represent dispersion. Curves representing $n_1\omega_1+n_2\omega_2$, $n_1\omega_1-n_2\omega_2$, and $n_2\omega_2-n_1\omega_1$ are shown in Figs. 4(b) and 4(c). Two types of behavior are shown for $n_1\omega_1+n_2\omega_2$, which produce different types of MS. More complicated dispersion than that shown in Fig. 4 could occur near absorption bands. The horizontal dashed lines represent possible values of $n_3\omega_3$. The intersections of the curves with $n_3\omega_3$ (shown as crosses) correspond to collinear processes. Whenever $n_3\omega_3$ satisfies

$$|n_1\omega_1-n_2\omega_2|<n_3\omega_3<n_1\omega_1+n_2\omega_2, \tag{47}$$

noncollinear processes are possible satisfying (43). The range of ω_1 over which (47) can be satisfied is indicated by shading for each choice of $n_3\omega_3$. The topology of the MS and foci is indicated by symbols on the left together with arrows showing the range in $n_3\omega_3$ which each symbol applies. In these symbols the foci are heavy dots, the MS is one or two closed curves, and the collinear processes are indicated as crosses corresponding to the crosses on the dashed lines.

Three types of MS are indicated in Fig. 4: (A) having one sheet between the foci with the foci excluded; (B) having one sheet with the foci included; and (C) having two sheets with a focus included in each sheet. These are the types of MS expected in highly transparent crystals. Normal dispersion is the case shown in Fig. 4(c); the case shown in Fig. 4(b) requires anomalous dispersion, but for sufficiently small ω_1 this is always present in polar crystals due to the strong lattice absorption in the infrared. Thus, both types of dispersion shown in Fig. 4 can be expected in the same crystal, that of Fig. 4(b) for relatively low pump frequency ω_3 and that of Fig. 4(c) for relatively high ω_3. If the dispersion is more complicated and $n_1\omega_1+n_2\omega_2$ has more than one extremum (maximum or minimum), the MS will have more sheets, the topology of which can easily be deduced in any particular case.

For an analytical description of these cases it is convenient to write

$$\omega_1=\omega_0+\Delta\omega, \quad \omega_2=\omega_0-\Delta\omega, \tag{48}$$

where $2\omega_0=\omega_3$, and $\Delta\omega$ satisfies the condition

$$0\leq(\Delta\omega)^2\leq\omega_0^2. \tag{49}$$

For moderate dispersion $n(\omega)$ can be expanded:

$$n(\omega)=n_0+(\omega-\omega_0)n'+\tfrac{1}{2}(\omega-\omega_0)^2n''+\tfrac{1}{6}(\omega-\omega_0)^3n'''+\cdots. \tag{50}$$

It follows that

$$n_1\omega_1+n_2\omega_2=n_0\omega_3+2(n'+\tfrac{1}{2}\omega_0n'')(\Delta\omega)^2+(\tfrac{1}{3}n'''+\tfrac{1}{12}\omega_0n'''')(\Delta\omega)^4+\cdots \tag{51}$$

and

$$n_1\omega_1-n_2\omega_2=2(n_0+\omega_0n')(\Delta\omega)+(n''+\tfrac{1}{3}\omega_0n''')(\Delta\omega)^3+\cdots. \tag{52}$$

For $|\Delta\omega|\ll\omega_0$, the solution of (51) and (44) is

$$(\Delta\omega)^2=\omega_0(n_3-n_0)/(n'+\tfrac{1}{2}\omega_0n'') \quad (\mathrm{FW}, |\Delta\omega|\ll\omega_0). \tag{53}$$

It is not expected that (52) and (45) or (46) would have a solution with $|\Delta\omega|\ll\omega_0$. When $|\Delta\omega|\sim\omega_0$, the approximate solution of (44) and (51) is

$$(\Delta\omega)^2=\omega_0^2(n_3-n_0)/[n(\omega_3)-n_0] \quad (\mathrm{FW}, |\Delta\omega|\sim\omega_0) \tag{54}$$

obtained by the use of (50) after replacing $(\Delta\omega)^4\rightarrow\omega_0^2(\Delta\omega)^2$ in (51). Similarly, the solution of (45) and (52) can be written

$$\Delta\omega=\omega_0n_3/n(\omega_3) \quad (\mathrm{BW}, |\Delta\omega|\sim\omega_0), \tag{55}$$

which is expected to hold whenever the BW solution exists.

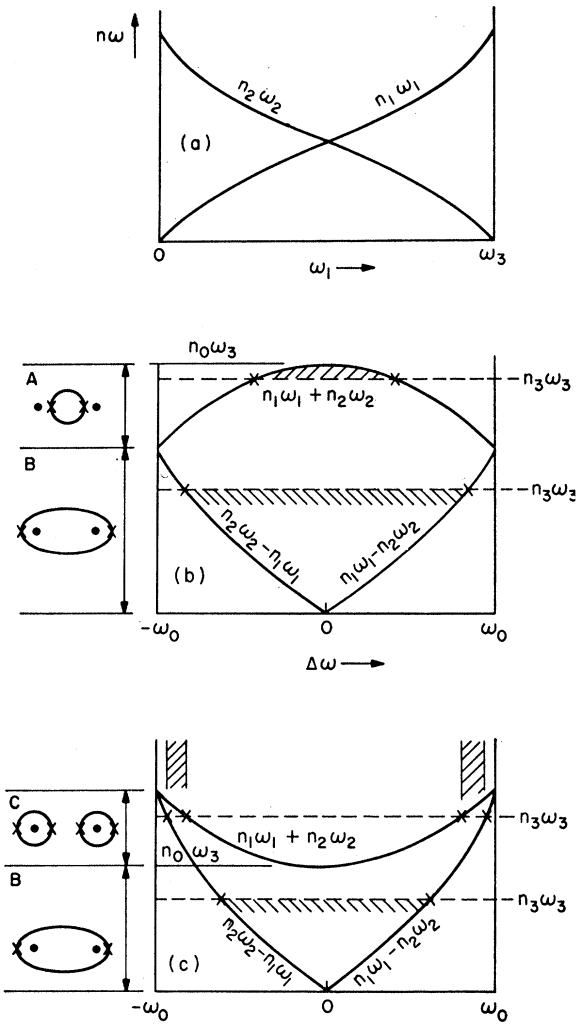

FIG. 4. Deduction of the possible types of matching surface from consideration of collinear processes. (a) Schematic plots of $n_1\omega_1$ and $n_2\omega_2$. (b) Plots of $n_1\omega_1+n_2\omega_2$ and $|n_1\omega_1\pm n_2\omega_2|$ with the collinear processes (44)–(46) indicated by crosses. Corresponding matching surfaces are shown by symbols A, B. (c) Similar to (b) with a different dispersive behavior leading to another type C of matching surface. Shaded regions denote the range in $\Delta\omega$ of non-collinear processes.

The conditions for the types of MS in Fig. 4 can now be written in the following forms:

$$\text{(A)} \quad \omega_0(n'+\tfrac{1}{2}\omega_0n'')<n_3-n_0<0 \quad (|\Delta\omega|\ll\omega_0) \tag{56}$$

or

$$n(\omega_3)<n_3<n_0 \quad (|\Delta\omega|\sim\omega_0), \tag{57}$$

$$\text{(B)} \quad n_3<n(\omega_3), \quad n_3<n_0 \quad (|\Delta\omega|\sim\omega_0), \tag{58}$$

$$\text{(C)} \quad 0<n_3-n_0<(n'+\tfrac{1}{2}\omega_0n'')\omega_0 \quad (|\Delta\omega_{\mathrm{FW}}|\ll\omega_0) \tag{59}$$

or

$$0<n_3-n_0<n(\omega_3)-n_0 \quad (|\Delta\omega_{\mathrm{FW}}|\sim\omega_0). \tag{60}$$

Here, $\Delta\omega_{\mathrm{FW}}$ denotes a solution of (44). Note that in (A) the BW solution does not exist, in (B) the FW does not exist, but in (C) both FW and BW exist.

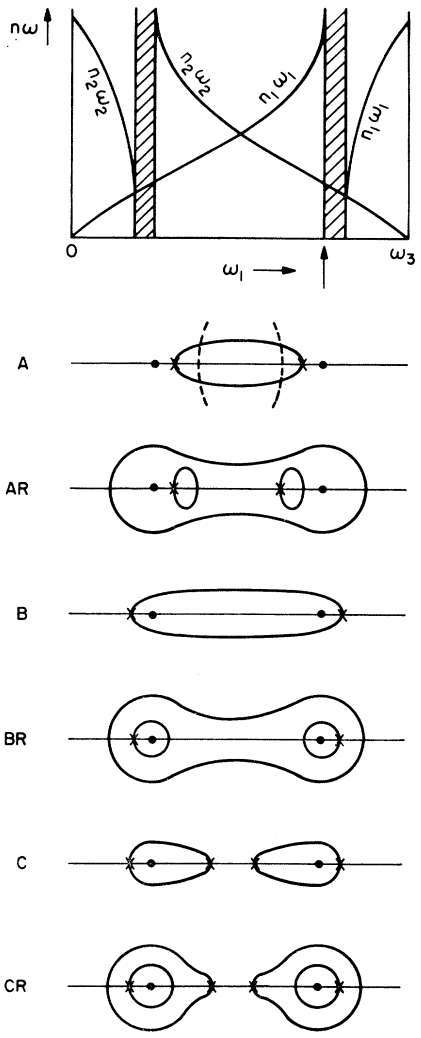

FIG. 5. Effects of a strong absorption on the matching surface. Polariton dispersion curves are shown for $n_1\omega_1$ and $n_2\omega_2$. Resonance in ω_1 is indicated by arrow; the forbidden frequency gap is shaded. Dashed circles centered on the foci in the symbol for type A represent the resonance. The actual matching surface taking the resonance into account is shown by symbols AR, BR, CR. Collinear processes present without resonance are shown by crosses.

The MS for the degenerate case $n_3=n_0$ can be either a single point at $\theta=0$, $\Delta\omega=0$ or else a continuous curve crossing itself like a figure eight on its side with each loop enclosing one focus. Consider an MS of type A in Fig. 4(b), and let n_3 increase until $n_3=n_0$. The single sheet of type A shrinks to a point as $n_3\rightarrow n_0$; for $n_3>n_0$ matching is impossible. Now consider types C and B in Fig. 4(c); as $n_3\rightarrow n_0$ the two sheets of C touch each other and the single sheet of B narrows down at the waist. In the symmetry plane $\Delta\omega=0$, it follows from (43) that

$$\text{(A,B)} \qquad \cos\theta=n_3/n_0 \quad (\Delta\omega=0), \tag{61}$$

which requires the MS to pinch off completely when $n_3=n_0$. Eventually, in the limit $n_3=n_0$, each of the curves C and B becomes a figure eight on its side with a focus in each loop. When $|\Delta\omega|\ll\omega_0$, (43) can be solved for θ as follows:

$$1-\cos\theta=(\omega_1n_1+\omega_2n_2-\omega_3n_3)/2\omega_1n_1 \quad (|\Delta\omega|\ll\omega_0). \tag{62}$$

When $n_3=n_0$, (62) and (51) lead to the relation

$$\theta=\pm[(2n'+\omega_0n'')/n_0\omega_0]^{1/2}(\Delta\omega) \quad (|\Delta\omega|\ll\omega_0), \tag{63}$$

which specifies the shape of the MS at the degenerate crossover. This shape may also be expressed in terms of the angle α between the MS and the z (pump beam) direction

$$\begin{aligned}\tan\alpha&=\pm[n_0\omega_0(2n'+\omega_0n'')]^{1/2}/(n_0+\omega_0n')\\&\approx\pm(\omega_3n'/n_0)^{1/2}.\end{aligned} \tag{64}$$

The width of the MS in Fig. 3 and the symbols of Fig. 4 have been greatly exaggerated for pictorial purposes. It is difficult to present a realistic plot of the MS because θ in practice is limited to a few degrees. The value of the MS is to aid in understanding the nature of phase-matched processes. The information of interest in experiments is most conveniently presented in the *collinear tuning curve*,[1–4,9] a plot of $\Delta\omega$ for the FW process (44) versus n_3, and the *noncollinear tuning characteristic*,[5,9] which is a plot of $\Delta\omega$ versus θ. In the collinear tuning curve, it is customary to present the crystal orientation or crystal temperature as the independent variable, but these parameters enter the theory through n_3. Collinear and noncollinear tuning have been extensively studied in ADP by Magde, Scarlet, and Mahr[3] and by Giallorenzi and Tang[9]; the latter have also made extensive calculations for $LiNbO_3$. All three types of MS shown in Fig. 4 have been found in these studies.

A weak absorption within the frequency range of the MS (shaded regions of Fig. 4) causes a resonance-type wiggle in the MS if the resonance frequency falls in the noncollinear part of the MS (between the crosses in the shaded regions). When the resonance falls close to a FW or BW process, a small extra-closed loop may be split off from the MS at this point (and also at the reflected point in the reflection plane $\Delta\omega=0$). More interesting effects are produced by a strong absorption. Figure 5 shows $n_1\omega_1$ and $n_2\omega_2$ with a strong sharp resonance. The shaded regions represent forbidden regions of frequency in the polariton dispersion[7] associated with the resonance. If damping is neglected, $n_1\omega_1$ can become arbitrarily large as the resonance (indicated by vertical arrow on ω_1 abscissa) is approached from below. The MS can be deduced by plotting $n_1\omega_1\pm n_2\omega_2$ as in Fig. 4. These plots will not be shown, but the resulting MS are sketched in Fig. 5. The top symbol A is a MS of type A with dashed circles centered on the foci to represent the position of the resonance. The effect of the resonance is shown in AR. The FW points (crosses) are little affected by the resonance; the pro-

found effect is to produce three sheets of one sheet by splitting off the ends of the original MS and stretching the main body around each focus. The part encircling the focus is approximately a circle. Also shown are MS of types B and C and the corresponding resonance types BR, CR.

6. BACKGROUND OPN

There is always present a background radiation in all directions due to processes for which $\Delta k \neq 0$. This emission is spread over a very broad band $0<\omega_1\leq\omega'(\theta)$, where $\omega'(\theta)$ is the limit frequency, which depends on direction as shown in Fig. 2. We see from (25), however, that the spectrum of the background is strongly weighted toward the high-frequency limit by the factor ω_1^4; additional weighting is provided by $|v_{2z}|^{-1}$, since $v_{2z}=0$ at the limit $\omega=\omega'$. The factor $\sin^2(\frac{1}{2}\Delta kl)$ may be replaced by its average value $\frac{1}{2}$. The general nature of the background spectrum can be illustrated with the aid of the rather drastic assumption

$$\begin{aligned} n_1=n_2=n=\text{const}, \\ n\neq n_3. \end{aligned} \tag{65}$$

With this assumption, all collinear processes ($\theta=0$) have the same $\Delta k=(n_3-n)\omega_3/c$. More generally, for $\mathbf{k}$ at angle θ, we have

$$\begin{aligned} \Delta k_\pm &= (n\omega_3/c)[A(\zeta,\theta)\pm D(\zeta,\theta)], \\ \zeta &\equiv \omega_1/\omega_3, \\ A(\zeta,\theta) &\equiv n_3/n-\zeta\cos\theta, \\ D(\zeta,\theta) &\equiv [1-2\zeta+\zeta^2\cos^2\theta]^{1/2}. \end{aligned} \tag{66}$$

The ($\pm$) in (66) corresponds to the two allowed $\mathbf{j}$ processes satisfying (1) and (23). The limit surface is given by

$$\omega'(\theta)=\omega_3/(1+\sin\theta). \tag{67}$$

It can be shown that

$$\begin{aligned} |v_{2z}| &= (c/n)D(\zeta,\theta)/(1-\zeta), \\ D(\zeta',\theta) &= 0, \\ \zeta'(\theta) &= \omega'(\theta)/\omega_3. \end{aligned} \tag{68}$$

The background OPN can now be written

$$\Delta\mathcal{P}_1=\Delta\nu_1\Delta\Omega_1(32\pi\chi^2\mathcal{P}_3\hbar\omega_3^3/n_3n^2c^3)S(\zeta,\theta), \tag{69}$$

where

$$S(\zeta,\theta)\equiv\frac{(A^2+D^2)(1-\zeta)^2\zeta^4}{(A^2-D^2)^2D}. \tag{70}$$

This includes both ($\pm$) processes of (66) under the assumption that the same χ^2 can be used for both. This is a reasonable assumption since the (+) process is unimportant except when the two $\mathbf{j}$ vectors are nearly equal. Thus, in (69), χ^2 should be chosen for the (−) process. Note that (69) does not contain the crystal length l.

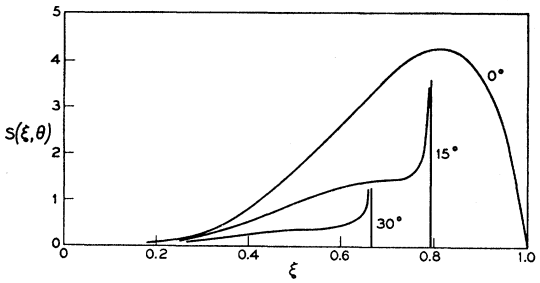

FIG. 6. The function $S(\xi,\theta)$, defined in (48) with $\xi=\omega_1/\omega_3$, gives the spectrum of the nonmatched background radiation. Shown are curves for $\theta=0°$, 15°, and 30°. The curves for 15° and 30° show the singularity with vertical edge at the limit frequency.

The interesting properties of the background are contained in $S(\zeta,\theta)$. Figure 6 shows $S(\zeta,\theta)$ as a function of ζ for $\theta=0°$, 15°, and 30°. Only the curve for 0° depends much on the value chosen for n_3/n; the curves were computed for $n_3/n=1.1$. For $\theta\neq 0$ there is a sharp peak with a vertical edge at $\zeta=\zeta'$. This peak is due to D^{-1} in (70) and represents the effect of $|v_{2z}|^{-1}$ in (25).

If the background spectrum can be observed, it may be of interest to have an expression for the integrated power under the peak. We may obtain the power by integrating (69) over ζ:

$$\begin{aligned} \frac{\Delta\mathcal{P}_1}{\Delta\Omega_1} &= \frac{16\chi^2\mathcal{P}_3\hbar\omega_3^4}{n_3n^2c^3}J(\theta), \\ J(\theta) &= \int S(\zeta,\theta)d\zeta \\ &= \int S(\zeta,\theta)\left(\frac{dD}{d\zeta}\right)^{-1}dD. \end{aligned} \tag{71}$$

From (66)

$$D\frac{dD}{d\zeta}=-1+\zeta\cos^2\theta. \tag{72}$$

We now replace the true $D(\zeta,\theta)$ with the stepwise linear approximation

$$\begin{aligned} &\zeta=\zeta', && \text{for } 0\leq D\leq 1-\zeta' \\ &\zeta=1-D, && \text{for } 1-\zeta'\leq D\leq 1. \end{aligned} \tag{73}$$

We may identify the peak with the first region. In $S(\zeta,\theta)$, we consider A a constant and D a variable. Thus the power of the peak is given by (71) with

$$\begin{aligned} J(\theta) &= \frac{(1-\zeta')^2(\zeta')^4}{1-\zeta'\cos^2\theta}\int_0^{1-\zeta'}dD\frac{A^2+D^2}{(A^2-D^2)^2} \\ &= \frac{(1-\zeta')^3(\zeta')^4}{(1-\zeta'\cos^2\theta)[A^2-(1-\zeta')^2]}. \end{aligned} \tag{74}$$

This does not include the broad shoulder on which the peak sits, which can readily be subtracted from the measured spectra if they have the shape predicted in Fig. 6.

7. SUMMARY

We have obtained the interaction energy (5) which couples three photons in an optically nonlinear medium. We have then formulated quantized fields at frequencies ω_1, ω_2, and $\omega_3=\omega_1+\omega_2$, and obtained the transition rate (18) for the decay of ω_3 into ω_1 and ω_2. This transition rate does not depend on the field distribution at ω_3; it can not be enhanced by focusing, and is independent of the position of the focus for a focused beam at ω_3.

We then assume a *plane wave* at ω_3 and obtained the power (25) emitted into band $\Delta\nu_1$ and solid angle $\Delta\Omega_1$. For any direction of emission there is a maximum limit frequency ω' sketched in Fig. 2. Phase-matched processes give narrow-band emissions with the power (27) and bandwidth (30). Emission tangential to the edge of the matching surface sketched in Fig. 3 gives greatly increased power (33) and a greatly broadened emission band (35). We have computed the total power (40) of phase-matched processes for the case $\omega_1\gg\omega_2$.

The nature of the matching surface and the different types to be expected have been discussed by considering the forward wave (44) and backward wave (45), (46) collinear processes. The types are indicated schematically for moderate dispersion in Fig. 4 and for resonance dispersion in Fig. 5.

Finally, we have sketched the spectrum of the background due to nonmatched processes in Fig. 6. Except in the forward direction, this spectrum has a singularity and an abrupt drop to zero at $\omega_1=\omega'$. The background is independent of crystal length l, whereas phase-matched processes give peaks proportional to l^2 and integrated powers proportional to l. An expression (74) has been given for the integrated power in the peak of the background spectrum. The expressions given for OPN apply only to the case of low parametric gain.

It must also be emphasized that theoretical results derived under the assumption of a plane-wave pump apply only when *diffraction* due to the finite size of the beam or the crystal can be neglected. It is the neglect of diffraction that leads to (23), upon which so much depends in the theory given here. The condition for the validity of treating the pump as a plane wave is derived in Appendix D. This condition can readily be met in practice.

ACKNOWLEDGMENTS

The author has benefited from discussions of various aspects of this work with C. H. Henry, R. G. Smith, L. Kreuzer, J. A. Giordmaine, and M. Lax of Bell Laboratories, C. L. Tang of Cornell University, and S. E. Harris of Stanford University.

APPENDIX A: GROUP VELOCITY

In the standard treatments of crystal optics[20] it is customary to consider complex plane waves of infinite extent,

$$\mathbf{E}(\mathbf{r},t)=\mathbf{u}f(\mathbf{r},t)e^{i\mathbf{k}\cdot\mathbf{r}-i\omega t}, \tag{A1}$$

with $f(\mathbf{r},t)=$ const. One finds that the unit polarization vector $\mathbf{u}$ satisfies

$$\{n^2[\mathbf{1}-\mathbf{ss}]-\boldsymbol{\varepsilon}(\omega)\}\cdot\mathbf{u}=0, \tag{A2}$$

where $\boldsymbol{\varepsilon}(\omega)$ is the dielectric dyadic and n is the refractive index defined by

$$\mathbf{k}=(n\omega/c)\mathbf{s}, \quad |s|=1. \tag{A3}$$

The locus of points $n\mathbf{s}$ defines the index surface, and it can be shown[21] that the normal to this surface is in the direction of energy flow. This is the ray direction, and the speed of energy flow in this direction is the ray velocity. The ray velocity considered as a vector is not identical with the group velocity

$$\mathbf{v}=\nabla_k\omega(\mathbf{k}) \tag{A4}$$

unless the medium is nondispersive $\boldsymbol{\varepsilon}(\omega)=\boldsymbol{\varepsilon}=$ const. The standard treatments[14] of the group velocity do not take into account the anisotropy of a general real symmetric tensor $\boldsymbol{\varepsilon}(\omega)$.

The problem is approached most directly by considering the propagation of a field (A1) with $f(\mathbf{r},t)$ a slowly varying function of space and time compared with $\exp(i\mathbf{k}\cdot\mathbf{r}-i\omega t)$. Let the electric displacement $\mathbf{D}(\mathbf{r},t)$ be given by

$$\begin{aligned}&\mathbf{D}(\mathbf{r},t)=\int_0^\infty \mathbf{R}(\tau)\cdot\mathbf{E}(\mathbf{r},t-\tau)d\tau,\\ &\mathbf{R}(0)=\mathbf{R}(\infty)=0,\end{aligned} \tag{A5}$$

where $\mathbf{R}(\tau)$ is the dielectric response function of the medium. In general,

$$\boldsymbol{\varepsilon}(\omega)=\int_0^\infty \mathbf{R}(\tau)e^{i\omega\tau}d\tau, \tag{A6}$$

and it easily follows that

$$\begin{aligned}&\int_0^\infty \ddot{\mathbf{R}}(\tau)e^{i\omega\tau}d\tau=-\dot{\mathbf{R}}(0)-\omega^2\boldsymbol{\varepsilon}(\omega),\\ &\int_0^\infty \ddot{\mathbf{R}}(\tau)e^{i\omega\tau}\tau\,d\tau=2i\omega\left[\boldsymbol{\varepsilon}(\omega)+\tfrac{1}{2}\omega\frac{\partial}{\partial\omega}\boldsymbol{\varepsilon}(\omega)\right],\end{aligned} \tag{A7}$$

where $\dot{\mathbf{R}}=\partial\mathbf{R}/\partial\tau$. It follows from Maxwell's equations

[20] See, for example, M. Born and E. Wolf, *Principles of Optics* (Pergamon Press, London, 1959).

[21] G. D. Boyd, A. Ashkin, J. M. Dziedzic, and D. A. Kleinman, Phys. Rev. 137, A1305 (1965); see especially the Appendix.

and (A5) that $\mathbf{E}(\mathbf{r},t)$ satisfies the wave equation

$$\nabla\times\nabla\times\mathbf{E}+c^{-2}\int_0^\infty \ddot{\mathbf{R}}(\tau)\cdot\mathbf{E}(t-\tau)d\tau + c^{-2}\dot{\mathbf{R}}(0)\cdot\mathbf{E}=0. \quad \text{(A8)}$$

We now substitute for $\mathbf{E}(\mathbf{r},t)$ from (A1). In the integral, we expand $f(\mathbf{r},t)$ in powers of τ:

$$f(\mathbf{r},t-\tau)=f(\mathbf{r},t)-\tau\dot{f}(\mathbf{r},t)+\cdots, \quad \text{(A9)}$$

dropping terms containing $\ddot{f}$ and higher time derivatives of f. In the first term of (A8) we drop space derivatives of f higher than ∇f. We also assume that $\mathbf{u}$ satisfies (A2). This leads to the following equation for $f(\mathbf{r},t)$:

$$[(\mathbf{k}\cdot\mathbf{u})\mathbf{1}+\mathbf{ku}-2\mathbf{uk}]\cdot\nabla f = \frac{2\omega}{c^2}\left[\left(\boldsymbol{\varepsilon}+\tfrac{1}{2}\omega\frac{\partial}{\partial\omega}\boldsymbol{\varepsilon}\right)\cdot\mathbf{u}\right]\dot{f}=0. \quad \text{(A10)}$$

We seek a solution in the form

$$f(\mathbf{r},t)=f(\mathbf{r}-\mathbf{v}t), \quad \text{(A11)}$$

where the *group velocity* $\mathbf{v}$ is to be determined by (A10). According to (A11),

$$\dot{f}=-\mathbf{v}\cdot\nabla f, \quad \text{(A12)}$$

so that (A10) becomes

$$\left[(\mathbf{k}\cdot\mathbf{u})\mathbf{1}+\mathbf{ku}-2\mathbf{uk}+\frac{2\omega}{c^2}\left(\boldsymbol{\varepsilon}+\tfrac{1}{2}\omega\frac{\partial}{\partial\omega}\boldsymbol{\varepsilon}\right)\cdot\mathbf{uv}\right]\cdot\nabla f=0. \quad \text{(A13)}$$

Since f is an arbitrary function, this requires that the dyadic in [ ] must vanish; it then follows immediately that

$$\mathbf{v}=\frac{\mathbf{k}-\mathbf{u}(\mathbf{k}\cdot\mathbf{u})}{\mathbf{u}\cdot(\boldsymbol{\varepsilon}+\frac{1}{2}\omega(\partial\boldsymbol{\varepsilon}/\partial\omega))\cdot\mathbf{u}}\cdot\frac{c^2}{\omega}. \quad \text{(A14)}$$

The time-averaged Poynting vector is

$$\mathbf{S}=(c/8\pi)\mathbf{E}\times\mathbf{H}^*, \quad \text{(A15)}$$

where $\mathbf{E}$ and $\mathbf{H}$ are time-independent amplitudes defined as in (4). For a plane wave,

$$\mathbf{H}=n\mathbf{s}\times\mathbf{E}, \quad \text{(A16)}$$

and $\mathbf{S}$ may be written

$$\mathbf{S}=(8\pi)^{-1}[\mathbf{E}(\mathbf{r})^*\cdot(\boldsymbol{\varepsilon}+\tfrac{1}{2}\omega(\partial\boldsymbol{\varepsilon}/\partial\omega))\cdot\mathbf{E}(\mathbf{r})]\mathbf{v}, \quad \text{(A17)}$$

where $\mathbf{v}$ is given by (A14). The instantaneous electric energy density is

$$U(\mathbf{r},t)_e=(4\pi)^{-1}\int_0^D \mathbf{E}\cdot d\mathbf{D}=(4\pi)^{-1}\int_{-\infty}^t \mathbf{E}\cdot\frac{\partial\mathbf{D}}{\partial t}dt. \quad \text{(A18)}$$

We write the real field in the form (4)

$$\mathbf{E}(\mathbf{r},t)=e^{at}\,\mathrm{Re}[\mathbf{E}(\mathbf{r})e^{-i\omega t}], \quad \text{(A19)}$$

with $a>0$ arbitrarily small to allow the field to be turned on adiabatically. The time-averaged electric energy density $U(\mathbf{r})_e$ is obtained by dropping terms in (A18) which vary as $\exp(\pm 2i\omega t)$:

$$U(\mathbf{r})_e=(8\pi)^{-1}\int_{-\infty}^t dt\,e^{2at}\int_0^\infty d\tau\,\mathbf{E}^*\cdot\mathbf{R}(\tau)\cdot\mathbf{E}(a\cos\omega\tau+\omega\sin\omega\tau)e^{-a\tau}. \quad \text{(A20)}$$

The integral exists in the limit $a\to 0$ only if $\boldsymbol{\varepsilon}(\omega)$ is real, which implies that

$$\int_0^\infty \mathbf{R}(\tau)\cos\omega\tau d\tau=\boldsymbol{\varepsilon}(\omega),$$
$$\int_0^\infty \mathbf{R}(\tau)\sin\omega\tau d\tau=0, \quad \text{(A21)}$$
$$\int_0^\infty \mathbf{R}(\tau)\sin\omega\tau e^{-a\tau}d\tau=a\frac{\partial}{\partial\omega}\boldsymbol{\epsilon}(\omega).$$

Thus, (A20) becomes

$$U(\mathbf{r})_e=(16\pi)^{-1}\mathbf{E}(\mathbf{r})^*\cdot\left[\boldsymbol{\varepsilon}(\omega)+\omega\frac{\partial}{\partial\omega}\boldsymbol{\varepsilon}(\omega)\right]\cdot\mathbf{E}(\mathbf{r}). \quad \text{(A22)}$$

The magnetic energy density is from (A16) and (A2),

$$U(\mathbf{r})_m=(16\pi)^{-1}|\mathbf{H}(\mathbf{r})|^2=(16\pi)^{-1}\mathbf{E}(\mathbf{r})^*\cdot\boldsymbol{\varepsilon}(\omega)\cdot\mathbf{E}(\mathbf{r}). \quad \text{(A23)}$$

The total time-averaged energy density is, therefore,

$$U(\mathbf{r})=U(\mathbf{r})_e+U(\mathbf{r})_m=(8\pi)^{-1}\mathbf{E}(\mathbf{r})^*\cdot(\boldsymbol{\varepsilon}+\tfrac{1}{2}\omega(\partial\boldsymbol{\varepsilon}/\partial\omega))\cdot\mathbf{E}(\mathbf{r}). \quad \text{(A24)}$$

It follows from (A17) and (A24) that the Poynting vector for a plane wave may be written

$$\mathbf{S}=U\mathbf{v}. \quad \text{(A25)}$$

For a wave packet (A1) with $f(\mathbf{r}-\mathbf{v}t)$ a slowly varying function (A25) is still a very good approximation.

It follows from (A14) that

$$\mathbf{u}\cdot(\boldsymbol{\varepsilon}+\tfrac{1}{2}\omega(\partial\boldsymbol{\varepsilon}/\partial\omega))\cdot\mathbf{u}=(nc/v)[1-(\mathbf{u}\cdot\mathbf{s})^2], \quad \text{(A26)}$$

where $v\equiv\mathbf{v}\cdot\mathbf{s}$. Thus, (A24) can be written for a plane wave

$$U=(nc/8\pi v)|E|^2, \quad \text{(A27)}$$

where E is the *transverse* component of $\mathbf{E}$:

$$E=|E|[1-(\mathbf{u}\cdot\mathbf{s})^2]^{1/2}. \quad \text{(A28)}$$

It remains to be shown that (A4) and (A14) are equivalent. It follows from (A2) that

$$(\omega/c)^2\delta\mathbf{u}\cdot\boldsymbol{\varepsilon}\cdot\mathbf{u}=(\omega/c)^2\mathbf{u}\cdot\boldsymbol{\varepsilon}\cdot\delta\mathbf{u} \\ =-(\mathbf{u}\cdot\mathbf{k})(\mathbf{k}\cdot\delta\mathbf{u}) \tag{A29}$$

for any variation $\delta\mathbf{u}$ satisfying $\delta\mathbf{u}\cdot\mathbf{u}=0$. Also, from (A2),

$$2\mathbf{k}\cdot\delta\mathbf{k}-2(\mathbf{k}\cdot\mathbf{u})(\mathbf{u}\cdot\delta\mathbf{k}+\mathbf{k}\cdot\delta\mathbf{u})=(2\omega/c^2)\delta\omega\mathbf{u}\cdot\boldsymbol{\varepsilon}\cdot\mathbf{u} \\ +(\omega/c)^2[\mathbf{u}\cdot\delta\boldsymbol{\varepsilon}\cdot\mathbf{u}+2\delta\mathbf{u}\cdot\boldsymbol{\varepsilon}\cdot\mathbf{u}] \tag{A30}$$

for an arbitrary variation $\delta\mathbf{k}$ which produces variations $\delta\mathbf{u}$, $\delta\omega$, and $\delta\boldsymbol{\varepsilon}$. Combining (A29) and (A30) gives

$$[\mathbf{k}-(\mathbf{k}\cdot\mathbf{u})\mathbf{u}]\cdot\delta\mathbf{k}=\delta\omega\frac{\omega}{c^2}\left[\mathbf{u}\cdot\left(\boldsymbol{\varepsilon}+\tfrac{1}{2}\omega\frac{\partial}{\partial\omega}\boldsymbol{\varepsilon}\right)\cdot\mathbf{u}\right], \tag{A31}$$

which can be written

$$\delta\omega=\mathbf{v}\cdot\delta\mathbf{k}, \tag{A32}$$

with $\mathbf{v}$ given by (A14). Since $\delta\mathbf{k}$ is an arbitrary variation, (A32) is identical with (A4).

APPENDIX B: OPN FROM NOISE WAVES

As mentioned in the Introduction, OPN has been ascribed[1,2,5] to the parametric amplification of fictitious "noise waves" having a power $h\nu_1 d\nu_1$ in bandwidth $d\nu_1$, and also to mixing[4] of the pump ω_3 with noise waves $h\nu_2 d\nu_2$ (one photon per mode at ω_2). These treatments are inconsistent in that no explanation has been (or can be) given why one mechanism should be invoked while neglecting the other. The answer obtained is in doubt because we may ask why both mechanisms should not operate simultaneously. A further inconsistency in the parametric amplification approach is that the parametric gain familiar from the paper of Louisell, Yariv, and Siegman[22] applies to the case of perfect phase matching; more generally it applies if the wave vector mismatch is less than the parametric gain. At low gain such as we are considering here, the bandwidth $\Delta\nu$ for such perfect phase matching would be negligibly small and not at all related to the actual bandwidth (30). Tien[23] has shown that, when the mismatch is larger than the gain parameter, the solutions for two waves coupled to a pump are periodic (sines and cosines) rather than exponential (hyperbolic sines and cosines). In this Appendix, a consistent description will be given of the parametric interaction of two "noise waves" E_k, ω_1 and E_j, ω_2 with a pump wave E_3, ω_3 which satisfy (1) and (23).

The vector field (8) satisfies the vector wave equation

$$\nabla\times\nabla\times\mathbf{E}-(\omega^2/c^2)\boldsymbol{\varepsilon}(\omega)\cdot\mathbf{E}=4\pi(\omega^2/c^2)\mathbf{P}, \tag{B1}$$

where $\boldsymbol{\varepsilon}(\omega)$ is the dielectric constant tensor and $\mathbf{P}$ is the polarization (3) at frequency ω. With E_k, E_j, E_3 the transverse amplitudes and χ the effective nonlinear coefficient (9), the equation for $E_k(z)$ (considered a slowly varying function of z) becomes

$$e^{-i\mathbf{k}\cdot\mathbf{r}}\mathbf{u}_1\cdot\nabla\times\nabla\times(\mathbf{u}_1E_ke^{i\mathbf{k}\cdot\mathbf{r}})-(\omega_1^2/c^2)(\mathbf{u}_1\cdot\boldsymbol{\varepsilon}\cdot\mathbf{u}_1)E_k \\ =(4\pi\omega_1^2/c^2)\chi E_3E_j^*[1-(\mathbf{u}_1\cdot\mathbf{s}_1)^2]e^{i\Delta kz}. \tag{B2}$$

Here, Δk is defined in (22) and use has been made of (23). By neglecting second derivatives of $E_k(z)$ and using (A2) this can be reduced to the form

$$[\mathbf{u}_1(\mathbf{k}\cdot\mathbf{u}_1)-\mathbf{k}]\cdot\nabla E_k=-2\pi i(\omega_1/c)^2 \\ \times[1-(\mathbf{u}_1\cdot\mathbf{s}_1)^2]\chi E_3E_j^*. \tag{B3}$$

It follows from (A14) and (A26) that

$$\mathbf{u}(\mathbf{k}\cdot\mathbf{u})-\mathbf{k}=(\omega n/cv)[1-(\mathbf{s}\cdot\mathbf{u})^2]\mathbf{v}. \tag{B4}$$

Therefore the coupled equations for $E_k(z)$, $E_j(z)$ are[24]

$$\frac{dE_k}{dz}=-\frac{2\pi i\omega_1v_1}{cn_1v_{1z}}\chi E_3E_j^*e^{i\Delta kz}, \\ \frac{dE_j}{dz}=-\frac{2\pi i\omega_2v_2}{cn_2v_{2z}}\chi E_3E_k^*e^{i\Delta kz}. \tag{B5}$$

It will simplify notation slightly to assume that $v_z>0$. These equations take crystal anisotropy and dispersion properly into account through the components $v=\mathbf{v}\cdot\mathbf{s}$ and $v_z=\partial\omega/\partial k_z$ of the group velocity $\mathbf{v}$.

The solution of (B5) for given initial values $E_k(0)$, $E_j(0)$ is

$$E_k(z)e^{-1/2i\Delta kz}=E_k(0)[\cos\gamma z-(i\Delta k/2\gamma)\sin\gamma z] \\ +E_j(0)^*[-2\pi i(\omega_1v_1/c\gamma n_1v_{1z})\chi E_3\sin\gamma z], \tag{B6}$$

where

$$\gamma^2=(\tfrac{1}{2}\Delta k)^2-\alpha^2\geq 0, \\ \alpha^2=(4\pi^2\chi^2\omega_1\omega_2v_1v_2/c^2n_1n_2v_{1z}v_{2z})|E_3|^2. \tag{B7}$$

If $E_k(0)$, $E_j(0)$ represent noise amplitudes, there will be no interference (cross term) between these fields in the average intensity proportional to $|E_k(z)|^2$. Furthermore, the observable OPN at ω_1 will be proportional to $|E_k(z)|^2-|E_k(0)|^2$. From (B6) and (B7), OPN will be proportional to

$$|E_k(l)|^2-|E_k(0)|^2=[|E_k(0)|^2 \\ +(\omega_1v_1v_{2z}n_2/\omega_2v_2v_{2z}n_1)|E_j(0)|^2] \\ \times(\alpha/\gamma)^2\sin^2\gamma l, \tag{B8}$$

where now $z=l$, the crystal thickness. The first term of (B8) comes from the first term of (B6) which may be interpreted as the *parametric amplification* term. The second term of (B8) comes from the second term of (B6), which may be interpreted as the *mixing* term.

Assume that the noise energy in mode $\mathbf{k}$ is $g_1\hbar\omega_1$ and that in mode $\mathbf{j}$ is $g_2\hbar\omega_2$. The zero-point energy corre-

[22] W. H. Louisell, A. Yariv, and A. E. Siegman, Phys. Rev. **124**, 1646 (1961).
[23] P. K. Tien, J. Appl. Phys. **29**, 1347 (1958).
[24] (B5) differs slightly from Eq. (4.9) of Ref. 10; the latter are obtained by making the approximations $v_1/v_{1z}\approx k/k_z$, $v_2/v_{2z}\approx j/j_z$.

sponds to

$$g_1=g_2=\tfrac{1}{2}\quad\text{(zero-point energy)}. \tag{B9}$$

Rather than invoke (B9) immediately, it is instructive to retain g_1 and g_2 temporarily as independent parameters. Since the number of modes $\mathbf{k}$ in an interval $\Delta\nu_1\Delta\Omega_1$ is $\Delta\nu_1\Delta\Omega_1(L^3n_1^2\omega_1^2/4\pi^2c^2v_1)$, it follows from (12) that $|E_k(0)|^2$ may be written

$$|E_k(0)|^2=\Delta\nu_1\Delta\Omega_1(2g_1\hbar\omega_1^3n_1/\pi c^3), \tag{B10}$$

and a similar relation exists for $|E_j(0)|^2$. To express $\Delta\nu_2\Delta\Omega_2$ in terms of $\Delta\nu_1\Delta\Omega_1$, consider elements of volume $d\mathbf{k}$, $d\mathbf{j}$ in $\mathbf{k}$ and $\mathbf{j}$ space, respectively, with $\mathbf{k}$, $\mathbf{j}$ satisfying (1) and (23). It can easily be shown that

$$d\mathbf{j}=d\mathbf{k}|\,\partial\mathbf{j}/\partial\mathbf{k}|=d\mathbf{k}|\,(v_{1z}/v_{2z})|\,, \tag{B11}$$

where $|\partial\mathbf{j}/\partial\mathbf{k}|$ is the Jacobian between the $\mathbf{j}$ and $\mathbf{k}$ spaces. Thus,

$$\Delta\nu_2\Delta\Omega_2=\Delta\nu_1\Delta\Omega_1(n_1^2\omega_1^2v_2v_{1z}/n_2^2\omega_2^2v_1v_{2z}) \tag{B12}$$

and

$$|E_j(0)|^2=\Delta\nu_1\Delta\Omega_1(2g_2\hbar\omega_1^2\omega_2n_1^2v_2v_{1z}/\pi c^3n_2v_1v_{2z}). \tag{B13}$$

From (A25), (A27), and the assumption that $\mathbf{k}_3$ has only a z component,

$$|E_3|^2=L^{-2}(8\pi/cn_3)\mathcal{P}_3. \tag{B14}$$

The OPN power $\Delta\mathcal{P}_1$ in $\Delta\nu_1\Delta\Omega_1$ is

$$\Delta\mathcal{P}_1=L^2(n_1c/8\pi v_1)v_{1z}(|E_k(l)|^2-|E_k(0)|^2). \tag{B15}$$

From (B8), (B10), (B13), and (B14), this reduces to

$$\Delta\mathcal{P}_1=\Delta\nu_1\Delta\Omega_1\frac{8\pi\mathcal{P}_3\hbar}{n_3c^5}\frac{\chi^2n_1v_2\omega_1^4\omega_2}{n_2v_{2z}}(g_1+g_2)\frac{\sin^2\gamma l}{\gamma^2}. \tag{B16}$$

The assumption $v_{2z}>0$ could be removed by considering solutions of (B5) in which the initial value is regarded as $E_j(l)$ instead of $E_j(0)$. The result is simply to replace v_{2z} by $|v_{2z}|$ in (B16). For $\alpha^2\ll(\frac{1}{2}\Delta k)^2$, (B7) gives $\gamma^2=(\frac{1}{2}\Delta k)^2$. Thus, (B16) agrees with (25) if

$$g_1+g_2=1. \tag{B17}$$

In particular, the zero-point energy (B9) satisfies this condition and has the property that the amplification and mixing contributions are equal.

Although quite arbitrary, the procedure of setting $g_1=1$, $g_2=0$ will give the correct OPN in (B16). OPN then appears as the parametric amplification of noise waves having one photon ($\hbar\omega_1$) per mode. Similarly, one may arbitrarily set $g_1=0$, $g_2=1$ and ascribe OPN to mixing with noise waves having one photon ($\hbar\omega_2$) per mode. It would seem more meaningful physically to use (B9) and treat the modes $\mathbf{k}$ and $\mathbf{j}$ symmetrically with zero-point energy in each.

APPENDIX C: HARMONIC GENERATION

The purpose of this appendix is to verify that the interaction (5), field quantization (14), and transition rate (18) give the correct second harmonic generation. Let

$$E_1(\mathbf{r})=E_1f(\mathbf{r}),\qquad \int_V|f(\mathbf{r})|^2d\mathbf{r}=V \tag{C1}$$

be the laser transverse-field amplitude according to (4) and (8). The laser power, according to (15), is

$$\mathcal{P}_1=\hbar\omega_1(v_1/L)N, \tag{C2}$$

where N is the average photon number. Let

$$E_2(r)=\sum E_ke^{i\mathbf{k}\cdot\mathbf{r}},\qquad |k|=n_2\omega_2/c,\qquad \omega_2=2\omega_1, \tag{C3}$$

be the harmonic field. The field commutation relations (14) in this notation become

$$[E_k,E_{k'}{}^\dagger]=(8\pi\hbar\omega_2v_2/cn_2V)\delta_{kk'},\qquad [E_1,E_1{}^\dagger]=(8\pi\hbar\omega_1v_1/cn_1V). \tag{C4}$$

The nonlinear polarization (3) specialized to harmonic generation is

$$\mathbf{P}_2(\mathbf{r})=\mathbf{d}\cdot\mathbf{E}_1(\mathbf{r})\mathbf{E}_1(\mathbf{r}), \tag{C5}$$

and the interaction (5) reduces to

$$\begin{aligned}H'&=-\tfrac{1}{4}d\int_W d\mathbf{r}[E_1(\mathbf{r})E_1(\mathbf{r})E_2(\mathbf{r})^*+\text{c.c.}]\\&=-\tfrac{1}{4}\sum_k d[f^2(\mathbf{k})E_1E_1E_k{}^\dagger+\text{c.c.}],\end{aligned} \tag{C6}$$

where d is the effective (harmonic) nonlinear coefficient, and

$$f^2(\mathbf{K})\equiv\int_W d\mathbf{r}[f(\mathbf{r})]^2e^{-i\mathbf{K}\cdot\mathbf{r}}. \tag{C7}$$

The transition $|N,0\rangle\rightarrow|N-2,1\rangle$ creates a photon in state $\mathbf{k}$ and destroys two photons from the state $f(\mathbf{r})$. The rate (18) for this transition is

$$\begin{aligned}R&=(2\pi/\hbar^2)\delta(\omega_2-2\omega_1)|\langle 0,N|H'|N-2,1\rangle|^2\\&=\frac{2^6\pi^4}{c^3n_1^2L^7}\mathcal{P}_1^2d^2|f^2(\mathbf{k})|^2\frac{v_2\omega_2}{n_2}\delta(2\omega_1-\omega_2).\end{aligned} \tag{C8}$$

For a plane-wave pump in the z direction,

$$|f^2(\mathbf{k})|^2=(2\pi L)^2\delta(k_x)\delta(k_y)[\sin^2\tfrac{1}{2}\Delta kl/(\tfrac{1}{2}\Delta k)^2], \tag{C9}$$

where

$$\Delta k=n_1\omega_2/c-k_z. \tag{C10}$$

The harmonic power is

$$\mathcal{P}_2=(2\pi)^{-3}V\int dk_xdk_ydk_z\,\hbar\omega_2R. \tag{C11}$$

The result is most conveniently written in terms of the intensities $S_1=\mathcal{P}_1/L^2$ and $S_2=\mathcal{P}_2/L^2$:

$$S_2=\frac{32\pi^3\omega_2^2d^2}{c^3n_1^2n_2}S_1^2\frac{\sin^2\frac{1}{2}\Delta kl}{(\frac{1}{2}\Delta k)^2}, \tag{C12}$$

which is known[11] to be the correct result for plane waves normal to the crystal surface.

This result can also be obtained quickly from (B5), which in the present notation is

$$\frac{dE_2}{dz}=-\frac{2\pi i\omega_2v_2}{cn_2v_{2z}}dE_1^2e^{i\Delta kz}, \tag{C13}$$

with Δk as in (C10). Since (23) requires $\mathbf{k}$ to have only a z component, we have $v_2=v_{2z}$, $v_1=v_{1z}$, and

$$|E_1|^2=(8\pi/n_1c)S_1, \quad |E_2|^2=(8\pi/n_2c)S_2. \tag{C14}$$

(C12) now follows immediately from (C13) and (C14).

APPENDIX D: FINITE BEAMS

In practice, the laser beam is not a plane wave but has a finite cross section. The most convenient representation for such a beam is the Gaussian beam[17,21,25] (or focused beam)

$$E_3(x,y,z)=E_0\frac{1}{1+i\xi}e^{ik_3z}\exp\left[-\frac{x^2+y^2}{w_0^2(1+i\xi)}\right], \tag{D1}$$

where

$$\xi=2(z-f)/b, \qquad b=w_0^2k_3. \tag{D2}$$

For convenience, we have assumed that the pump is an *ordinary wave* in a uniaxial crystal. The focus is at $x=y=0$, $z=f$, the minimum beam radius is w_0, the confocal parameter is b, and the far-field diffraction half-angle is

$$\delta_0=2w_0/b=2/w_0k_3=\lambda_3/\pi w_0, \tag{D3}$$

with λ_3 being the wavelength in the medium. The power in the beam is

$$\mathcal{P}_3=(\tfrac{1}{16}n_3c)w_0^2|E_0|^2 \tag{D4}$$

if the variation of n_3 over the angle spread δ_0 can be neglected. In the notation of (10), the field operator for the beam can be taken to be

$$E_3\equiv E_0 \tag{D5}$$

and the normalized beam function $f(\mathbf{r})$ is then

$$f(\mathbf{r})=(2/\pi)^{1/2}\frac{L}{w_0}\frac{1}{1+i\xi}e^{ik_3z}\exp\left[-\frac{x^2+y^2}{w_0^2(1+i\xi)}\right]. \tag{D6}$$

The Fourier components (17) can easily be evaluated with the result

$$|f(\mathbf{K})|^2=2\pi w_0^2L^2\exp[-\tfrac{1}{2}w_0^2(K_x^2+K_y^2)]\times\sin^2\tfrac{1}{2}\Delta k'l/(\tfrac{1}{2}\Delta k')^2, \tag{D7}$$

where

$$\Delta k'\equiv k_3-K_z-(K_x^2+K_y^2)/2k_3. \tag{D8}$$

The transition rate (18) for OPN depends upon $|f(\mathbf{k}+\mathbf{j})|^2$, obtained by setting $\mathbf{K}=\mathbf{k}+\mathbf{j}$ in (D7) and (D8). It is easily verified that (D7) approaches (21) in the limit $w_0\to\infty$. Note that (D7) is independent of the position f of the focus.

The OPN power $\Delta\mathcal{P}_1$ in $\Delta\nu_1\Delta\Omega_1$ is obtained by substituting (D7) into (20) with $\mathbf{K}=\mathbf{k}+\mathbf{j}$. If it be assumed that χ, n_1, v_2, etc., have the values appropriate for a plane-wave pump, the result can be written

$$\Delta\mathcal{P}_1=\Delta\nu_1\Delta\Omega_1\frac{8\pi\mathcal{P}_3\hbar}{n_3c^5}\frac{\chi^2n_1v_2\omega_1^4\omega_2}{n_2|v_{2z}|}\left\langle\frac{\sin^2\frac{1}{2}\Delta k'l}{(\frac{1}{2}\Delta k')^2}\right\rangle, \tag{D9}$$

where $\langle\ \rangle$ denotes the average

$$\langle F(\eta)\rangle\equiv e^{-\gamma^2}\int_0^\infty d\eta\, I_0(2\gamma\eta^{1/2})e^{-\eta}F(\eta),$$
$$\gamma=2^{1/2}(v_{2x}^2+v_{2y}^2)^{1/2}/|v_{2z}|\delta_0, \tag{D10}$$
$$I_0(z)\equiv(2\pi)^{-1}\int_0^{2\pi}e^{-z\cos\theta}d\theta\equiv J_0(iz),$$

$\Delta k'(\eta)$ is the function

$$\Delta k'(\eta)=\Delta k+[k_3(v_{2x}^2+v_{2y}^2)/2v_{2z}^2]-(\eta/b_0), \tag{D11}$$

and Δk is the mismatch (22) for a plane-wave pump. From the power-series expansion of $I_0(z)$ (Bessel function of imaginary argument of order zero), it can easily be shown that

$$\int_0^\infty d\eta\, e^{-\eta}I_0(2\gamma\eta^{1/2})=e^{\gamma^2}. \tag{D12}$$

From this, by differentiation with respect to γ, it can be shown that

$$\langle\eta\rangle=1+\gamma^2, \qquad \langle(\eta-\langle\eta\rangle)^2\rangle=1+2\gamma^2. \tag{D13}$$

Thus the rms deviation of $\Delta k'(\eta)$ about its mean value is

$$\langle(\Delta k'(\eta)-\langle\Delta k'\rangle)^2\rangle^{1/2}=b_0^{-1}(1+2\gamma^2)^{1/2}. \tag{D14}$$

The mean mismatch is

$$\langle\Delta k'(\eta)\rangle=\Delta k-b_0^{-1}. \tag{D15}$$

The *criterion* for the validity of the plane-wave approximation is that the rms deviation of $\Delta k'(\eta)$ should be small compared to the effective band of emission given in terms of Δk by (29). Thus we obtain the criterion

$$\pi b_0\gg l(1+2\gamma^2)^{1/2}. \tag{D16}$$

[25] G. D. Boyd and J. P. Gordon, Bell System Tech. J. **40**, 489 (1961).

For nearly *collinear* processes, we can go a step further by noting that

$$(v_{2x}^2+v_{2y}^2)^{1/2}/|v_{2z}| = \tan\rho_2 \approx \rho_2, \qquad \gamma = 2^{1/2}\rho_2/\delta_0, \tag{D17}$$

where ρ_2 is the double-refraction angle for the **j** photon. The criterion (D16) is then equivalent to the two criteria

$$\pi b_0 \gg l, \qquad \pi b_0 \gg 2l\rho_2/\delta_0. \tag{D18}$$

For noncollinear processes, γ is nonvanishing even if $\rho_2=0$. As $|v_{2z}| \to 0$, γ becomes large but (D10) breaks down in this limit. The criteria (D18) are readily satisfied in practice. Note that the second criterion is essentially equivalent to

$$l \ll l_a,$$

where $l_a=\pi^{1/2}\rho_2/w_0$ is the aperture length [see Eq. (3.41) of Ref. 21] of the pump (with the pump considered to have double-refraction angle ρ_2). Note that in this case (pump an ordinary wave) the relevant value of ρ is that of the unobserved photon **j**.

When the pump is an *extraordinary wave* in a uniaxial crystal, the relevant double-refraction angle is $|\rho_2-\rho_3|$. Let the optic axis be in the xz plane. Then x in (D6) becomes $x-\rho_3(z-f)$, and K_z in (D8) becomes $K_z+\rho_3 K_x$. The final result has the form (D10), with

$$\gamma = 2^{1/2}[(v_{2x}-\rho_3|v_{2z}|)^2+v_{2y}^2]^{1/2}/|v_{2z}|\delta_0. \tag{D19}$$

For nearly *collinear* processes, $v_{2y}\approx 0$ and $v_{2x}\approx\rho_2|v_{2z}|$, so that (D19) reduces to

$$\gamma = 2^{1/2}|(\rho_2-\rho_3)|/\delta_0 \tag{D20}$$

and (D18) is replaced by

$$\pi b_0 \gg l, \qquad \pi b_0 \gg 2l|\rho_2-\rho_3|/\delta_0, \tag{D21}$$

which includes (D18) as a special case. Thus we see that the *relative* double-refraction angle between the pump and **j** photon is significant in the plane-wave approximation.

PHYSICAL REVIEW VOLUME 174, NUMBER 3 15 OCTOBER 1968

Debye-Waller Factors in Rare-Gas Solids*

VICTOR V. GOLDMAN
Rutgers—The State University, New Brunswick, New Jersey 08903
(Received 17 June 1968)

Mean-square amplitudes for inert-gas solids neon, argon, krypton, and xenon have been calculated as a function of temperature. The results are presented for the cases of zero pressure and constant volume. A nearest-neighbor (m-6) Mie-Lennard-Jones potential was used, and lowest-order anharmonic contributions were taken into account by the frequency-shift method.

I. INTRODUCTION

RECENT experiments on the Mössbauer effect in solid krypton[1,2] in addition to measurements of the elastic neutron scattering in solid neon[3] have yielded measurements of the Debye-Waller factor as a function of temperature. In this paper the mean-square nuclear displacement is calculated as a function of temperature for the rare-gas crystals neon, argon, krypton, and xenon. Anharmonic effects are included by using the approximate frequency-shift method.[4,5] The calculations are based on an (m-6) Mie-Lennard-Jones central force potential, with interactions between nearest neighbors only. This model has been successful in accounting for other properties of rare-gas crystals.[6]

II. THEORY

The substances we are considering assume an fcc Bravais lattice and for these the Debye-Waller factor, which in the Mössbauer effect describes the temperature dependence of the fraction of recoilless transitions, can be expressed as[7]

$$M = e^{-k^2\langle u^2\rangle/3},$$

where k is the wave number of the emitted γ ray and

* Work supported by U. S. Air Force Office of Scientific Research under Grant No. AFOSR 68-1372.

[1] K. Gilbert (private communication).

[2] M. Pasternak, A. Simopoulos, S. Bukshpan, and T. Sonnino, Phys. Letters **22**, 52 (1966).

[3] D. G. Henshaw, Phys. Rev. **111**, 1470 (1958).

[4] T. H. K. Barron, in *Lattice Dynamics* (Pergamon Press, Inc., New York, 1965), p. 247.

[5] J. L. Fledman, G. K. Horton, and J. B. Lurie, J. Phys. Chem. Solids **26**, 1507 (1965).

[6] G. K. Horton, Am. J. Phys. **36**, 93 (1968).

[7] A. Abragam, *L'effet Mössbauer* (Gordon and Breach Science Publishers Inc., New York, 1964). We have neglected "anomalous" terms due to anharmonicity which lead to anisotropy in the Debye-Waller factor. These have been shown to be quite small in general (see Ref. 8).